energy&fuels

Article

pubs.acs.org/EF

Kinetic Model of Steam Gasification of Biomass in a Bubbling Fluidized Bed Reactor

Bijan Hejazi,* John R. Grace, Xiaotao Bi, and Andrés Mahecha-Botero†

Department of Chemical and Biological Engineering, University of British Columbia, 2360 East Mall, Vancouver, British Columbia V6T 1Z3, Canada

ABSTRACT: A simple kinetic model is developed for biomass gasification in a bubbling fluidized bed (BFB) with steam as the fluidizing gas. The biomass pyrolysis is described by a two-step kinetic model in which the primary pyrolysis is modeled by three parallel first-order reactions producing noncondensable gas, tar (bio-oil), and char, and the secondary pyrolysis is modeled by a first-order reaction representing homogeneous thermal cracking of tar. In addition to the yields of pyrolysis products that are often modeled as lumped species, the proportions of major compounds in the pyrolysis gas are predicted based on CHO elemental balances. By incorporating homogeneous and heterogeneous biomass gasification reactions, a seamless kinetic model of a BFB gasifier is developed. An ideal reactor model is used for the BFB gasifier assuming perfectly mixed solids and plug flow of the gas phase. This predictive model is a useful tool to relate biomass gasification product yields and composition to key process operating parameters such as biomass ultimate analysis, reactor temperature, and steam-to-biomass ratio. Predictions of the gasifier model are in good agreement with experimental data from the literature.

INTRODUCTION

Since approximately the 1850s, global use of fossil fuels (coal, oil, and natural gas) has dominated energy supply, leading to rapid increase in greenhouse gas (GHG) emissions. Some of the possible options to lower GHG emissions while still matching the global demand for energy services are energy conservation and efficiency, fossil fuel switching, renewable energy, nuclear, and carbon capture and storage (CCS). The share of renewable energy in the energy mix has substantially increased in recent years and is projected to increase substantially under most ambitious mitigation scenarios.[1] Among the renewable energy options is gasification of biomass. There is renewed interest in gasification, due in part to its ability to produce hydrogen as a clean energy carrier.[2]

Gasification is a high-temperature partial oxidation process in which a solid carbonaceous feedstock such as biomass is converted to gaseous products (in particular, H_2, CO, CO_2, CH_4, light hydrocarbons), as well as liquid tar (heavy hydrocarbons) and minor contaminants, by gasifying agents such as air, oxygen, steam, carbon dioxide, or their mixtures.[3] These agents produce synthetic gases of different calorific values. Steam gasification of biomass produces a medium heating value gas mixture, i.e., 10−18 MJ/Nm^3 higher heating value[3−6] (HHV), an attractive choice compared to lower heating value gases generated from air gasification (4−7 MJ/Nm^3, HHV).[4,7−9] Gasifying with pure steam also produces a higher hydrogen content of the product gas.[3,10]

Fluidized beds have a history of proven operability in the field of solid fuel conversion to gaseous products. Good heat and mass transfer, temperature uniformity, superior solid−gas contact, high solids flow rates, and great flexibility with regard to handling a variety of fuel quantity and quality relative to fixed beds are among their characteristics.[11] Biomass gasification in fluidized bed reactors is of both scientific and industrial significance, with an ongoing quest to enhance the economic feasibility of the process.

Previous reactor models of biomass gasifiers range from simple equilibrium models, useful for the overall estimation of the process,[4,12] to comprehensive kinetic models, which take into account a complicated network of kinetic reactions, mass and heat balances, and hydrodynamic constraints to predict species concentrations, solids hold up, and temperature profiles along the reactor.[13−16] Each type of model has its own strengths and limitations. Equilibrium models possess generic applicability for simulating different gasifier configurations as they are independent of gasifier design and not limited to a specified range of operating conditions. However, experimental results show that some gasification reactions do not reach equilibrium due to kinetic, heat transfer, and mass transfer limitations.[5,12,17,18] Kinetic models, on the other hand, are capable of estimating the composition of product gas with varying operating conditions, which is essential for designing, evaluating, and improving gasifiers. Nevertheless, a problem with kinetic models is that many of the reactions are catalyzed by solids, and the reaction kinetics are then dependent on metallic components of biomass ash and therefore difficult to represent accurately.

Due to its complexity, kinetic modeling of biomass gasifiers is at an early phase. Important information is missing from the fluidized bed gasifier kinetic model of Corella et al.,[13] mostly due to its proprietary nature. The kinetic model of Radmanesh et al.,[14] applied to a single bubbling fluidized bed gasifier, contains useful reaction kinetic information. Lü et al.[15] developed a kinetic model of biomass air−steam gasification in a fluidized bed reactor, assuming steady-state conditions and instantaneous pyrolysis. Kaushal et al.[16] also developed a comprehensive kinetic model for a bubbling fluidized bed

Received: November 29, 2016
Revised: January 10, 2017
Published: January 11, 2017

DOI: 10.1021/acs.energyfuels.6b03161
Energy Fuels 2017, 31, 1702−1711

gasifier. In developing these models, various simplifying assumptions were included for practical applications. For instance, while some assume instantaneous drying and pyrolysis, others consider the progression of these phenomena to be crucial components of the model.[16,19] Although the gasification product gas is often assumed to be free from tar,[20] some include a submodel for tar generation and cracking.[19] Furthermore, there is enormous diversity in reaction mechanisms and kinetic rate expressions in the biomass gasification literature. To support a reliable model, measurements of the gas composition and yield of pyrolysis in laboratory scale at high heating rates with the biomass of interest are required.[5] Nevertheless, for almost all engineering applications, researchers resort to fixed values or temperature-dependent experimental correlations for the composition of the pyrolysis gas.[21]

The objective of this paper is to develop a simple, yet practical, reactor model for predicting the performance of steam gasification of biomass in a bubbling fluidized bed. In our model, the incorporation of the two-step biomass pyrolysis kinetic mechanism, constrained by CHO elemental balances, allows for improving the predictions of pyrolysis products distribution. By defining tar as a mixture of carbon, hydrogen, and oxygen, uncertainties in tar measurement and analysis are addressed. In addition to kinetic parameters and fuel-related and process-related parameters, the only other model input parameters are tar and char elemental compositions from ultimate and proximate analyses. Unlike other models, this predictive model minimizes reliance on empirical correlations.

MODEL DEVELOPMENT

The transfer of heat to a biomass particle includes external heat transfer from the heating medium to the particle surface and internal transfer from the particle surface to its interior. A typical measure of the ratio of external to internal heat transfer resistances is the dimensionless Biot number defined for spherical particle as[22]

$$Bi = hR_P/k_B \quad (1)$$

where h is the overall external heat transfer coefficient, R_P is the particle radius, and k_B is the thermal conductivity of the biomass particle. Biot numbers significantly smaller than 1 indicate a substance as "thermally thin", i.e., that the internal heat conduction is much faster than the external heat transfer and uniform temperature can be assumed throughout the particle volume. Biot numbers much larger than 1 indicate "thermally thick" particles with considerable internal temperature gradients.[23]

Upon entering a fluidized bed gasifier, biomass particles are exposed to very high heating rates causing rapid increase of particle temperature, evaporation of moisture, and devolatilization into volatile matter that may constitute more than 80% of the original particle mass. The rest remains in the form of solid char, which is subsequently consumed in heterogeneous gasification reactions in the presence of an oxidizing agent such as air or steam. During biomass drying and pyrolysis, the gasifying agent may not reach the particle surface due to high evaporation and devolatilization fluxes, whereas during gasification, the gasifying agent from the bulk gas stream is transported to the char surface, where it reacts heterogeneously. Therefore, it is fair to model drying, pyrolysis, and gasification as consecutive processes.

Simplifying Assumptions. To develop a sufficiently accurate model for steam gasification of biomass in a bubbling fluidized bed (BFB) reactor, the following simplifying assumptions are adopted.

(1) The reactor operates under steady-state conditions.
(2) By means of cyclone recycling, bottom feeding of biomass, and a long freeboard region, solids entrainment is minimized. As biomass particles produce a low proportion of char and a large proportion of volatile matter, the char particles are consumed in the bed, and thus, entrainment of the char is neglected.[14,16,24]
(3) Uniform temperature and total pressure are assumed throughout the dense bed.[11]
(4) The solids in the BFB reactor are perfectly mixed,[16,25−28] and there is an even distribution of drying and pyrolysis products throughout the dense bed height.[16]
(5) Gases and volatiles are in plug flow inside the reactor.[16,25−28]
(6) The freeboard region of the BFB is modeled as a plug flow reactor.[14,16,24,27]
(7) The particles are thermally thin with instantaneous heat up to the reactor temperature.
(8) Pyrolysis involves a two-step process with primary and secondary pyrolysis described by three parallel heterogeneous reactions and a homogeneous tar cracking reaction, respectively.[27−33]
(9) First-order Arrhenius-type chemical reactions are assumed for pyrolysis.[27−33]
(10) The bed material sand particles are inert and do not catalyze reactions.[34]
(11) The ash plays a negligible role in catalyzing reactions.
(12) Chemical reaction is the rate-controlling mechanism for char gasification inside the bubbling fluidized bed.
(13) The ideal gas law applies for all volatiles (gas and bio-oil) released from biomass pyrolysis.
(14) For elemental balances, each species, including unreacted biomass, char, noncondensable gas, and tar, is treated as a homogeneous mixture of carbon, hydrogen, and oxygen. Other elements, including nitrogen and sulfur, are neglected due to their low concentrations.

Reaction Kinetics. As illustrated in Figure 1, the biomass pyrolysis products distribution is approximated from the generic two-step kinetic mechanism[29−31] with the primary pyrolysis modeled by three parallel first-order reactions producing noncondensable gas, tar, and char. The secondary pyrolysis is modeled by a first-order reaction producing noncondensable gas from thermal cracking of tar. The selected kinetic parameters for primary pyrolysis are adopted from Chan et al.,[31] who verified their pyrolysis model predictions with experimental results for lodgepole pine (wood) devolatilzation. Furthermore, the reaction kinetics equation of Boroson et al.[35] is used to model thermal cracking of tar (bio-oil) to

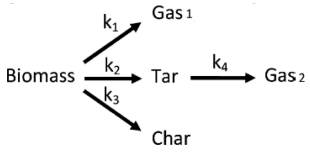

Figure 1. Two-step kinetic mechanism adopted for biomass pyrolysis.[29−31]

DOI: 10.1021/acs.energyfuels.6b03161
Energy Fuels 2017, 31, 1702−1711

noncondensable gas in the temperature range of 500−800 °C with the following stoichiometry

$$\text{Tar} \rightarrow \gamma_{CO}CO + \gamma_{CO_2}CO_2 + \gamma_{H_2}H_2 + \gamma_{CH_4}CH_4 + \gamma_{Tar_{inert}}Tar_{inert} \quad (2)$$

and the mass-based stoichiometric coefficients (γ_i)

$$\gamma_{CO} = 0.5633,\ \gamma_{CO_2} = 0.1109,\ \gamma_{H_2} = 0.0173,\ \gamma_{CH_4} = 0.0884,\ \gamma_{Tar_{inert}} = 0.22 \quad (3)$$

The above stoichiometry suggests that 78% of the primary tar is cracked, with the rest remaining unchanged. However, studies show that operating parameters, such as fluidizing agent, temperature, residence time, and ash, affect tar cracking.[16,36] To account for these effects, the yield of inert tar is assigned a zero value ($\gamma_{Tar_{inert}} = 0$), and the remaining yield is loaded on the noncondensable gas species

$$w_{CO,\text{tar cracking}} = \gamma_{CO}/(\gamma_{CO} + \gamma_{CO_2} + \gamma_{H_2} + \gamma_{CH_4}) = 0.7222 \quad (4)$$

$$w_{CO_2,\text{tar cracking}} = \gamma_{CO_2}/(\gamma_{CO} + \gamma_{CO_2} + \gamma_{H_2} + \gamma_{CH_4}) = 0.1422 \quad (5)$$

$$w_{CH_4,\text{tar cracking}} = \gamma_{CH_4}/(\gamma_{CO} + \gamma_{CO_2} + \gamma_{H_2} + \gamma_{CH_4}) = 0.1133 \quad (6)$$

$$w_{H_2,\text{tar cracking}} = \gamma_{H_2}/(\gamma_{CO} + \gamma_{CO_2} + \gamma_{H_2} + \gamma_{CH_4}) = 0.0222 \quad (7)$$

Table 1. Kinetic Parameters for Biomass Pyrolysis[a]

j	k_{0j} (1/s)	E_j (kJ/mol)	$\Delta H_{rxn,j}$ (kJ/kg)
1[b]	1.30×10^8	140	64
2[b]	2.00×10^8	133	64
3[b]	1.08×10^7	121	64
4[c]	1×10^5	93.3	−42

[a]For mechanism, see Figure 1. [b]Reference 31. [c]Reference 35.

All reaction rate constants are expressed in first-order and Arrhenius form as

$$k_j = k_{0j} \exp(-E_j/RT) \quad (8)$$

The kinetic parameters and heats of reaction are summarized in Table 1. In addition, the kinetic rate expressions of five major gasification reactions included in the model are listed in Table 2. Despite the wide variation of kinetic parameters reported for the same reaction, the set of reaction kinetics reported in Table 2 has been adopted after a thorough literature review. For different biomass feeds, the adopted heterogeneous char gasification reaction kinetic parameters are commonly used in the literature.[5,16] After analyzing models and kinetics from the literature, it is was found that it is better to consider the WGS reaction to be kinetically limited than at equilibrium.[5] Note that the catalytic effects of metal components present in the biomass ash, such as Ca, Na, and K, are not taken into account, despite reports that they can have a significant impact on the reaction network of biomass gasification.[34]

Reactor Model. For small biomass particles that meet the criterion of "thermally thin", evaporation of the moisture content, biomass devolatilization, and particle heat up to the reactor temperature all occur within seconds or almost instantaneously. Therefore, the yields of biomass pyrolysis products (per unit mass of dry biomass) are approximated at reactor temperature by

$$\bar{Y}_{G,pyro} = k_1/(k_1 + k_2 + k_3) \quad (9)$$

$$\bar{Y}_{T,pyro} = k_2/(k_1 + k_2 + k_3) \quad (10)$$

$$\bar{Y}_{C,pyro} = k_3/(k_1 + k_2 + k_3) \quad (11)$$

Assuming that tar, char, and noncondensable gas are homogeneous mixtures of carbon, hydrogen, and oxygen, the product gas composition is approximated from CHO elemental balances on the average particle experiencing pyrolysis inside the reactor. For a given reactor temperature, average elemental compositions are assigned to each lumped species and the particle mass balance is broken down into CHO elemental balances

Table 2. Major gasification reactions

	gasification reaction	reaction kinetic rate expression
Boudouard[37] [a]	$C(s) + CO_2 \rightarrow 2CO$ $\Delta H^0_{rxn} = +172$ kJ/mol	$r_{C1}(s^{-1}) = 3.1 \times 10^6 \exp\left(\frac{-21\,5000}{RT}\right) \times P^{0.38}_{CO_2}[\text{bar}]$
water−gas[38] [a]	$C(s) + H_2O \rightarrow CO + H_2$ $\Delta H^0_{rxn} = +131$ kJ/mol	$r_{C2}(s^{-1}) = 2.62 \times 10^8 \exp\left(\frac{-23\,7000}{RT}\right) \times P^{0.57}_{H_2O}[\text{bar}]$
methanation[39] [a]	$C(s) + 2H_2 \rightarrow CH_4$ $\Delta H^0_{rxn} = -75$ kJ/mol	$r_{C3}(s^{-1}) = 16.4 \exp\left(\frac{-94\,800}{RT}\right) \times P^{0.93}_{H_2}[\text{MPa}]$
steam methane reforming (SMR)[40]	$CH_4 + H_2O \leftrightarrow CO + 3H_2$ $\Delta H^0_{rxn} = +206$ kJ/mol	$r_{SMR}(\text{mol}\cdot\text{m}^{-3}\cdot\text{s}^{-1}) = 3 \times 10^5 \exp\left(\frac{-12\,5000}{R\cdot T}\right) \times C_{CH_4}\cdot C_{H_2O}$
water−gas shift (WGS)[41,42]	$CO + H_2O \leftrightarrow CO_2 + H_2$ $\Delta H^0_{rxn} = -41$ kJ/mol	$K_{WGS} = 0.0265 \exp\left(\frac{3968}{T}\right)$ $r_{WGS}(\text{mol}\cdot\text{m}^{-3}\cdot\text{s}^{-1}) = 2.78 \exp\left(\frac{-1510}{T}\right) \times \left(C_{CO}\cdot C_{H_2O} - \frac{C_{CO_2}\cdot C_{H_2}}{K_{WGS}}\right)$

[a]First-order reactions with respect to solid carbon. $R = 8.314$ J·mol^{-1}·K^{-1}, T in Kelvin, and C_i in mol·m^{-3}.

DOI: 10.1021/acs.energyfuels.6b03161
Energy Fuels 2017, 31, 1702−1711

$$w_{j,B} = \overline{Y}_{C,pyro}\cdot w_{j,C} + \overline{Y}_{T,pyro}\cdot w_{j,T} + \overline{Y}_{G,pyro}\cdot w_{j,G} \quad (j = C, H, O) \tag{12}$$

where the elemental composition of dry-ash-free biomass ($w_{j,B}$) is obtained from its ultimate analysis and char is approximated as pure carbon

$$w_{C,C} = 1;\quad w_{H,C} = 0;\quad w_{O,C} = 0 \tag{13}$$

Substituting pyrolysis product yields into eq 12 and solving for the elemental composition of tar released from the surface of biomass particles

$$w_{j,T} = ((k_1 + k_2 + k_3)\cdot w_{j,B} - k_1\cdot w_{j,G} - k_3\cdot w_{j,C})/k_2 \quad (j = C, H, O) \tag{14}$$

Note that the tar (bio-oil) product includes both organic compounds and water produced during pyrolysis of dry biomass. Although the tar derived from the pyrolysis of biomass is a complex mixture of low- and high-molecular-weight oxygenated compounds, such as carboxylic acids, aldehydes, ketones, alcohols, and phenols,[43] its dry-basis elemental composition is a very weak function of temperature.[44] As a model input parameter, we adopt the following empirical mass ratios for the organic constituents of tar[44]

$$w_{C,T,organic} = 1.14\cdot w_{C,B};\quad w_{H,T,organic} = 1.13\cdot w_{H,B};\quad w_{O,T,organic} = 1 - w_{C,T,organic} - w_{H,T,organic} \tag{15}$$

If $\overline{Y}_{H_2O,pyro}$ denotes the released pyrolytic water yield per mass of dry biomass, the overall tar (bio-oil) composition is related to its organic part elemental composition as

$$w_{j,T} = ((\overline{Y}_{T,pyro} - \overline{Y}_{H_2O,pyro})\cdot w_{j,T,organic} + \overline{Y}_{H_2O,pyro}\cdot w_{j,H_2O})/\overline{Y}_{T,pyro} \quad (j = C, H, O) \tag{16}$$

Solving for the pyrolytic water yield divided by the tar yield we obtain the following relationships between tar elemental compositions

$$\frac{\overline{Y}_{H_2O,pyro}}{\overline{Y}_{T,pyro}} = \frac{w_{C,T} - w_{C,T,organic}}{w_{C,H_2O} - w_{C,T,organic}} = \frac{w_{H,T} - w_{H,T,organic}}{w_{H,H_2O} - w_{H,T,organic}} = \frac{w_{O,T} - w_{O,T,organic}}{w_{O,H_2O} - w_{O,T,organic}} \tag{17}$$

With the assumption that the noncondensable pyrolysis gas is composed of four major compounds: H_2, CO, CO_2, and CH_4, with other light hydrocarbons (e.g., C_2 and C_3) lumped into methane, the average dry gas elemental composition from biomass pyrolysis is

$$w_{C,G} = (12/28)\cdot w_{CO,pyro} + (12/44)\cdot w_{CO_2,pyro} + (12/16)\cdot w_{CH_4,pyro} \tag{18}$$

$$w_{H,G} = (4/16)\cdot w_{CH_4,pyro} + w_{H_2,pyro} \tag{19}$$

$$w_{O,G} = (16/28).\ w_{CO,pyro} + (32/44)\cdot w_{CO_2,pyro} \tag{20}$$

Experimental evidence[31,44] shows that the hydrogen content of the noncondensable gas is almost negligible. Hence, we set

$$w_{H_2,pyro} \cong 0 \tag{21}$$

Given that each compound composition in pyrolysis gas must also fall between zero and unity, the following constraints apply

$$\begin{bmatrix} 0 < w_{H,G} < 0.25 \\ 0.2727 + 1.9091\cdot w_{H,G} < w_{C,G} < 0.4286 + 1.9091\cdot w_{H,G} \\ 0.5714 - 2.2857\cdot w_{H,G} < w_{O,G} < 0.7273 - 2.2857\cdot w_{H,G} \end{bmatrix} \tag{22}$$

Simultaneous solution of eqs 14 and 16 subject to the above constraints gives a range of acceptable results for tar and gas compositions as well as pyrolytic water yield released from the surface of biomass particles at different reactor temperatures.

In the reactor model, the gas and particle flows are treated separately. While perfect mixing provides a reasonable representation of solid mixing inside a bubbling fluidized bed reactor, the gas flow is closer to plug flow as shown schematically in Figure 2. The black circles in Figure 2 are a schematic

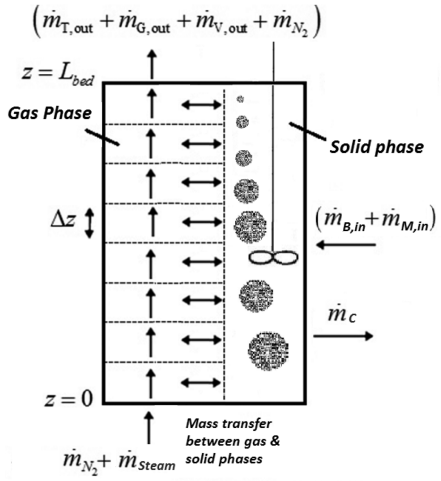

Figure 2. Reactor model schematic. CSTR for solids and PFR for gas.

representation of biomass/char particles that are perfectly mixed inside the solid phase of the dense bubbling bed.

Assuming plug flow of the gas phase and uniform distribution of drying and pyrolysis products throughout the entire dense bed height, L_{bed}, with uniform temperature, the one-dimensional tar (bio-oil) mass balance at height z of the bed with cell height (Δz) is written

$$\text{Tar: } \dot{m}_T(z) - \dot{m}_T(z + \Delta z) + \overline{Y}_{T,pyro}.\ \dot{m}_{B,in}.\ (\Delta z/L_{bed}) - k_4.\ (1 - \gamma_{Tar_{inert}})\cdot(\dot{m}_T(z).\ \Delta\tau_g) = 0 \tag{23}$$

The incremental gas residence time for a bed of cross-sectional area A is calculated from local bed voidage (ε) and superficial gas-phase velocity (U)

DOI: 10.1021/acs.energyfuels.6b03161
Energy Fuels 2017, 31, 1702−1711

$$\Delta\tau_g = \frac{\varepsilon \cdot A \cdot \Delta z}{U \cdot A} \tag{24}$$

where the local bed voidage (ε) is obtained from Clift and Grace[45]

$$\varepsilon = 1 - (1 - \varepsilon_{mf})/(1 + (U - U_{mf})/(0.711\sqrt{g \cdot d_b})) \tag{25}$$

and bubble size (d_b) is estimated as a function of height z in the bed from the correlation of Darton et al.[46]

$$d_b = 0.54 g^{-0.2}(U - U_{mf})^{0.4}(z + 4\sqrt{A/N_{or}})^{0.8} \tag{26}$$

Substituting $\Delta\tau_g$ into the tar mass balance and letting $\Delta z \to 0$

$$\text{Tar: } \frac{d\dot{m}_T}{dz} = \overline{Y}_{T,pyro} \cdot \dot{m}_{B,in}/L_{bed} - k_4 \cdot (1 - \gamma_{Tar_{inert}}) \cdot (\dot{m}_T(z) \cdot \varepsilon/U) \tag{27}$$

$$B.\ C.: \dot{m}_T|_{(z=0)} = 0$$

Similarly, one-dimensional differential equations are written for noncondensable gas species

$$\text{Dry Gas: } \frac{d\dot{m}_G}{dz} = \overline{Y}_{G,pyro} \cdot \dot{m}_{B,in}/L_{bed} + k_4 \cdot (1 - \gamma_{Tar_{inert}}) \cdot (\dot{m}_T(z) \cdot \varepsilon/U) + \frac{d\dot{m}_{G,gasification}}{dz} \tag{28}$$

$$B.\ C.: \dot{m}_G|_{(z=0)} = 0$$

The third term on the right side of eq 28 is the net rate of generation/consumption of gaseous species due to homogeneous and heterogeneous gasification reactions

$$\frac{d\dot{m}_{G,gasification}}{dz} = \frac{d\dot{m}_{CO,gasification}}{dz} + \frac{d\dot{m}_{CO_2,gasification}}{dz} + \frac{d\dot{m}_{CH_4,gasification}}{dz} + \frac{d\dot{m}_{H_2,gasification}}{dz} \tag{29}$$

If M_{Char} is the char hold up in the dense bed, according to major gasification reactions listed in Table 2

$$\frac{d\dot{m}_{CO,gasification}}{dz} = \left(\varepsilon \cdot (r_{SMR} - r_{WGS}) + (1 - \varepsilon) \cdot \frac{(M_{Char}/MW_{Char})}{(A \cdot L_{bed} \cdot (1 - \varepsilon))} \cdot (2 \cdot r_{C1} + r_{C2})\right) \cdot A \cdot MW_{CO} \tag{30}$$

$$\frac{d\dot{m}_{CO_2,gasification}}{dz} = \left(\varepsilon \cdot (r_{WGS}) + (1 - \varepsilon) \cdot \frac{(M_{Char}/MW_{Char})}{(A \cdot L_{bed} \cdot (1 - \varepsilon))} \cdot (-r_{C1})\right) \cdot A \cdot MW_{CO_2} \tag{31}$$

$$\frac{d\dot{m}_{CH_4,gasification}}{dz} = \left(\varepsilon \cdot (-r_{SMR}) + (1 - \varepsilon) \cdot \frac{(M_{Char}/MW_{Char})}{(A \cdot L_{bed} \cdot (1 - \varepsilon))} \cdot (r_{C3})\right) \cdot A \cdot MW_{CH_4} \tag{32}$$

$$\frac{d\dot{m}_{H_2,gasification}}{dz} = \left(\varepsilon \cdot (3 \cdot r_{SMR} + r_{WGS}) + (1 - \varepsilon) \cdot \frac{(M_{Char}/MW_{Char})}{(A \cdot L_{bed} \cdot (1 - \varepsilon))} \cdot (r_{C2} - 2 \cdot r_{C3})\right) \cdot A \cdot MW_{H_2} \tag{33}$$

Given $w_{i,pyro}$ and $w_{i,tar}$ cracking from elemental balances on the biomass particles during pyrolysis and the thermal tar cracking kinetic model, respectively, the mass balances for the individual gas species (i = CO, CO_2, CH_4, H_2) are

$$\frac{d\dot{m}_i}{dz} = \overline{Y}_{G,pyro} \cdot \dot{m}_{B,in}/L_{bed} \cdot w_{i,pyro} + k_4 \cdot (1 - \gamma_{Tar_{inert}}) \cdot (\dot{m}_T(z) \cdot \varepsilon/U) \cdot w_{i,tar\ cracking} + \frac{d\dot{m}_{i,gasification}}{dz} \tag{34}$$

$$B.\ C.: \dot{m}_i|_{(z=0)} = 0$$

The differential equation for the water vapor/steam mass balance is

$$\frac{d\dot{m}_{H_2O}}{dz} = \frac{\dot{m}_{M,in}}{L_{bed}} + \left(\varepsilon \cdot (-r_{SMR} - r_{WGS}) + (1 - \varepsilon) \cdot \frac{(M_{Char}/MW_{Char})}{(A \cdot L_{bed} \cdot (1 - \varepsilon))} \cdot (-r_{C2})\right) \cdot A \cdot MW_{H_2O} \tag{35}$$

$$B.\ C.: \dot{m}_{H_2O}|_{(z=0)} = \dot{m}_{Steam,in}$$

Given an initial guess for the char hold up of the dense bubbling bed, the above coupled ODEs are solved numerically to give the axial profiles of steam, tar, and noncondensable gas species mass flow rates along the reactor using the MATLAB ODE solver (ODE45).

The char hold up of the dense bubbling bed with a given mean solids residence time τ_P is updated by performing a char balance over the bed at steady state, with no char in the feed

$$\dot{m}_{Char,out} = \dot{m}_{Char,gen} - \dot{m}_{Char,cons} \tag{36}$$

where

$$\dot{m}_{Char,out} = M_{char}/\tau_P \tag{37}$$

$$\dot{m}_{Char,gen} = \overline{Y}_{C,pyro} \cdot \dot{m}_{B,in} \tag{38}$$

Fluidized bed particles are often small enough that internal resistances to transfer are small. External transfer resistances are also likely to be smaller than those related to chemical reaction. Furthermore, the small char particles are subject to severe fragmentation inside the bed. Therefore, it is reasonable to neglect the internal and external mass transfer resistances and assume that heterogeneous reactions are the rate-controlling mechanism for char gasification. The rate of char consumption due to heterogeneous gasification reactions is then approximated as (see Table 2)

$$\dot{m}_{Char,cons} = \int_0^{L_{bed}} (d\dot{m}_{Char,gasification}/dz) \cdot dz = \int_0^{L_{bed}} (r_{C1}(z) + r_{C2}(z) + r_{C3}(z)) \cdot (M_{char}/L_{bed}) \cdot dz \tag{39}$$

DOI: 10.1021/acs.energyfuels.6b03161
Energy Fuels 2017, 31, 1702−1711

Substituting the above values in the char balance equation

$$M_{char} = \bar{Y}_C \cdot \dot{m}_{B,in}/(1/\tau_p + \int_0^{L_{bed}} (r_{C1}(z) + r_{C2}(z) + r_{C3}(z)) \cdot dz/L_{bed}) \quad (40)$$

The local partial pressures and concentrations of gasifying species as well as superficial gas velocity at height z in the bed with uniform operating temperature (T) and total pressure (P) are estimated from gaseous species mass flow rates and the ideal gas law

$$y_i(z) = (\dot{m}_i(z)/MW_i)/\sum_i (\dot{m}_i(z)/MW_i)$$

$$(i = CO, CO_2, CH_4, H_2, H_2O, N_2, Tar) \quad (41)$$

$$P_i(z) = y_i(z) \cdot P \quad (42)$$

$$C_i(z) = P_i(z)/(R \cdot T) \quad (43)$$

$$U(z) = \left(\frac{R \cdot T}{P \cdot A}\right) \cdot \sum_i (\dot{m}_i(z)/MW_i) \quad (44)$$

Given the total bed inventory (W_{bed}) or the bed height (L_0) at minimum fluidization ($\varepsilon = \varepsilon_{mf}$), the height of the expanded dense bubbling bed (L_{bed}) is also obtained iteratively

$$W_{bed} = \rho_{sand} \cdot A \cdot L_{bed} \cdot (1 - \bar{\varepsilon}) = \rho_{sand} \cdot A \cdot L_0 \cdot (1 - \varepsilon_{mf}) \quad (45)$$

where the average bed voidage is calculated as

$$\bar{\varepsilon} = (\int_0^{L_{bed}} \varepsilon \cdot dz)/L_{bed} \quad (46)$$

Note that the assumptions of uniform total pressure, temperature, and solids hold up are reasonable approximations due to dispersion in the dense section of a bubbling fluidized bed reactor. The axial variations of temperature and pressure along the bed are taken into account by coupling ODE's describing energy and pressure balances along the bed. Neglecting the entrainment of char and sand particles, the freeboard region is modeled as an ideal plug flow reactor ($\varepsilon_{fb} = 1$) in which only tar cracking and homogeneous gasification reactions (SMR and WGS) take place. The boundary conditions for the ODE's describing the freeboard region are from the values obtained at the top of the dense bubbling bed.

RESULTS AND DISCUSSION

The predictions of the BFB gasifier model are compared with experimental results of Herguido et al.,[47] who studied the steam gasification of different types of biomass species in a BFB gasifier of 0.15 m internal diameter in the temperature range of 650−780 °C and steam-to-biomass ratios of 0.4−3. The properties of pine (sawdust and wood chips), as well as the experimental operating conditions used in their study, are summarized in Tables 3 and 4, respectively. In their experimental runs, the biomass flow rate was varied to provide the desired steam-to-biomass ratios at a constant steam volumetric flow rate.

Figures 3a and 3b illustrate the model predictions for yields of tar, dry nitrogen-free product gas, and char generated from steam gasification of pine sawdust in the BFB reactor as a function of steam-to-biomass and reactor temperature, respectively. As observed, the yields of gas are predicted to increase with increasing S/B ratio and reactor temperature, whereas tar and char yields decrease. Comparing model predictions with the experimental data, the char and tar yields

Table 3. Properties of Biomass Species Used in the Experimental Study[47]

type of pine	sawdust	wood chips
particle size	500 μm	2 × 5 × 10 mm
proximate analysis (wt % basis)		
moisture	8.5	11.1
ash	1.2	2.1
volatiles	77.4	74.4
fixed carbon	12.9	12.4
ultimate analysis (wt %)		
C	42.5	41.8
H	6.3	5.3
O	51	52.7
N	0.2	0.2
low heating value (MJ/kg daf)	18.8	18.5

Table 4. Gasifier Operating Conditions Used during the Experimental Study[47]

bed diameter	0.15 m
freeboard diameter	0.15 m
total column height	1.2 m
bed height (L_0) at $U_0 = U_{mf}$	0.32 m
fluidizing gas mixture	90% H_2O/10% N_2
reactor temperature	650−780 °C
total reactor pressure	1.1 atm
superficial gas velocity at inlet (U_0) at reactor temperature	0.25 m/s
biomass flow rate	3.94−3.46 kg/h
steam/biomass ratio	0.4−3
silica sand bed inventory	8 kg
average sand particle diameter	200−300 μm
sand particle density	2600 kg/m^3

are reasonably predicted, whereas the product gas yield is always overpredicted. This discrepancy may be attributed to the temperature drop in the freeboard and downstream equipment such as a cyclone, exit gas line, and heat exchanger that are externally heated and insulated. Our model predictions do not account for this temperature drop in the freeboard given the difficulty of estimating the contribution of the ovens and electrical resistances in the absence of overall heat balances in the original paper.[47] Some of the simplifying assumptions adopted to develop a predictive model could also contribute to the deviation of model predictions from experimental data. For instance, the limitations of the two-step pyrolysis kinetic model for different types of biomass with varying properties significantly affects the model predictions. Furthermore, to close the CHO elemental balances with minimum reliance on empirical correlations, the light hydrocarbons (e.g., C_2 and C_3) are lumped into methane. Finally, a more elaborate reaction network for tar reforming and cracking may improve the model predictions.

Figure 4 illustrates the effect of S/B ratio on dry and N_2-free product gas composition for steam gasification of pine sawdust at a reactor temperature of 750 °C. As expected, the H_2 mole fraction in the product gas increases with increasing S/B ratio because of the water−gas, steam methane reforming, and water−gas shift reactions. The CO_2 mole fraction also increases with increasing S/B ratio, probably due to the water−gas shift reaction that is dominant at high temperatures. Upon increasing the S/B ratio, the mole fractions of CO and CH_4 decrease due to enhanced WGS and SMR reactions. The model predictions for product gas composition are shown in Figure 5

DOI: 10.1021/acs.energyfuels.6b03161
Energy Fuels 2017, 31, 1702−1711

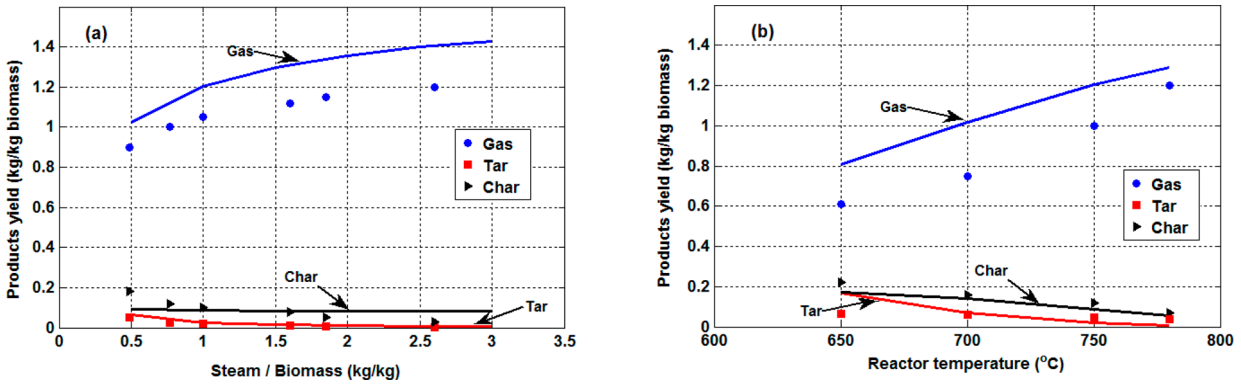

Figure 3. Predicted yield distribution of products from steam gasification of pine sawdust (lines) compared with experimental data from Herguido et al.[47] (points). (a) Effect of S/B ratio at a reactor temperature of 750 °C. (b) Effect of reactor temperature at a S/B ratio of 0.86.

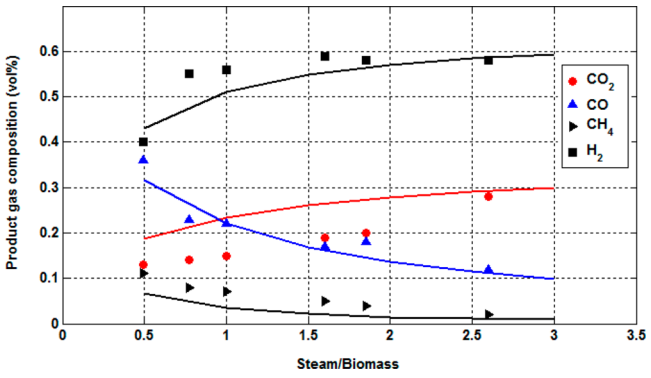

Figure 4. Effect of steam-to-biomass ratio on dry and N_2-free product gas composition for steam gasification of pine sawdust at a reactor temperature of 750 °C. Experimental data points are from Herguido et al.[47]

as a function of reactor temperature, together with experimental data for steam gasification of pine.[47] At higher temperatures, H_2 and CO production is promoted by endothermic Boudouard, water−gas, and steam methane reforming reactions. Furthermore, elevating the temperature reverses the exothermic WGS reaction toward more H_2 and CO production and CO_2 consumption. Note that the CO_2 mole fraction reported for sawdust pine[47] increases slightly with increasing temperature, which is inconsistent with other modeling and experimental data from the literature.[24,48] The product gas composition from steam gasification of pine wood chips in Figure 5 shows better agreement with the model predictions.

CONCLUSIONS

Steam gasification of biomass is modeled in a BFB reactor. On the basis of two-step pyrolysis kinetics constrained by elemental

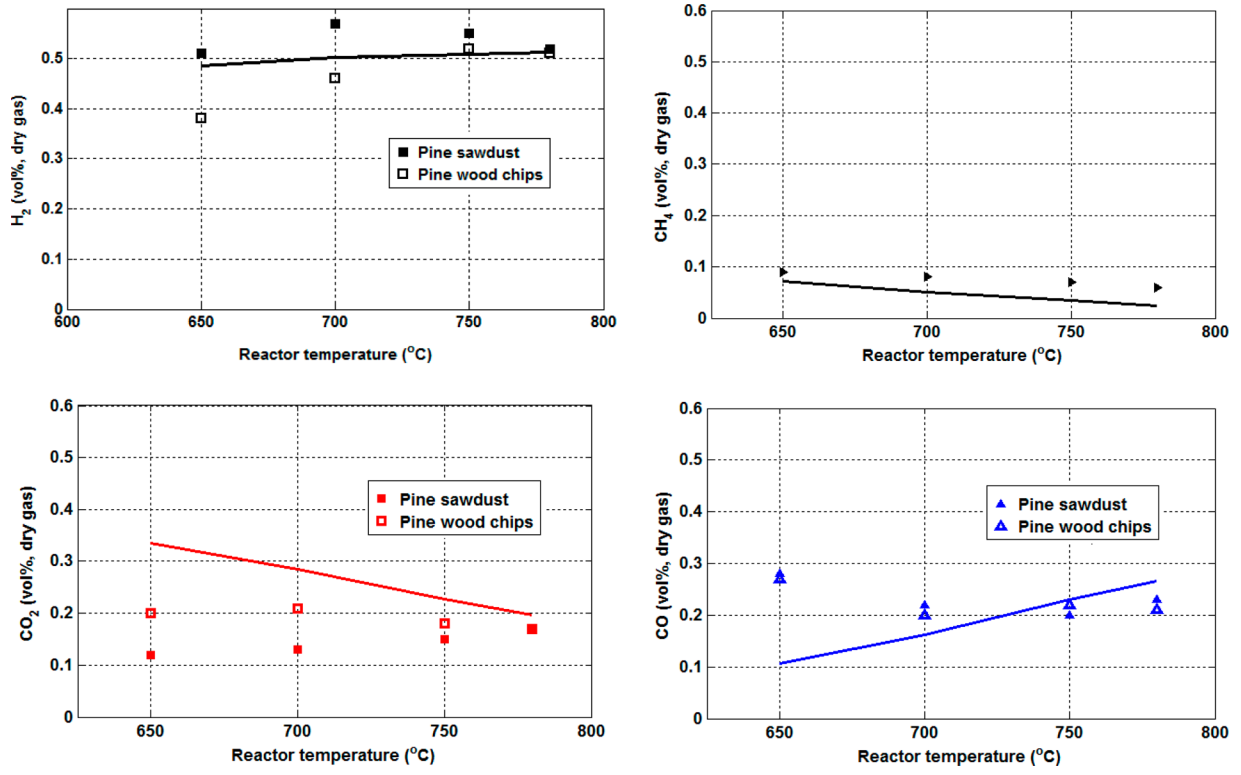

Figure 5. Effect of reactor temperature on dry N_2-free product gas composition for steam gasification of pine at a S/B ratio of 0.86. Lines are predictions from the model developed in this paper, and experimental data points are from Herguido et al.[47]

DOI: 10.1021/acs.energyfuels.6b03161
Energy Fuels 2017, 31, 1702−1711

balances, the model predicts major compounds composition in pyrolysis gas. The effects of steam-to-biomass ratio and reactor temperature on the distribution of products generated from steam gasification of pine sawdust and pine chips are predicted and compared with experimental data from the literature. The product gas composition from steam gasification of pine shows good agreement with the model predictions. The most important conclusions are as follows.

(1) The yields of gas increase, while tar and char yields decrease, with increasing steam-to-biomass (S/B) ratio or reactor temperature.
(2) The effect of S/B ratio on dry and N_2-free product gas composition for steam gasification of pine sawdust in a BFB reactor at a temperature of 750 °C showed that the H_2 mole fraction in the product gas increases with increasing S/B ratio because of the water−gas, steam methane reforming, and water−gas shift reactions. The CO_2 mole fraction also increases with increasing S/B ratio, probably due to the water−gas shift reaction becoming dominant at high gasifier temperatures. Increasing the S/B ratio causes the mole fractions of CO and CH_4 to decrease due to enhanced WGS and steam methane reforming (SMR) reactions.
(3) The predicted product gas composition for steam gasification of pine sawdust shows that at higher reactor temperatures, H_2 and CO production are promoted by the endothermic Boudouard, water−gas, and steam methane reforming reactions. Elevating the temperature also reverses the exothermic WGS reaction toward more CO production and CO_2 consumption.

The current model could be improved by the following.

(1) Applying a two-phase hydrodynamic model.
(2) Developing a 2D or 3D model to solve the problem of gas mixing.
(3) Accounting for temperature variations along the free-board region.
(4) Extending the application of the model by developing a single-particle model and coupling it to the reactor model.
(5) Accounting for the catalytic effect of ash with fuel-specific biomass gasification reaction kinetics.
(6) Using a more elaborate reaction mechanism for tar reforming and cracking.
(7) Utilizing improved kinetic tracking individual chemical species (no lumping).

AUTHOR INFORMATION

Corresponding Author

*Phone: 604-363-2481. E-mail: bijanhejazi@gmail.com; bhejazi@chbe.ubc.ca.

ORCID

Bijan Hejazi: 0000-0002-6912-7726

Present Address

†A.M.-B.: NORAM Engineering, 200 Granville Street, Suite 1800 Vancouver, British Coumbia V6C 1S4, Canada.

Notes

The authors declare no competing financial interest.

ACKNOWLEDGMENTS

The authors gratefully acknowledge financial aid from Carbon Management Canada and the Natural Sciences and Engineering Research Council of Canada.

NOMENCLATURE

A = bubbling bed cross-sectional area, m^2
Bi = Biot number, -
C_i = concentration of species i, mol/m^3
d_b = bubble size, m
E_j = activation energy of the jth reaction, kJ/mol
G = acceleration of gravity, 9.81 m^2/s
h = heat transfer coefficient, $W/m^2{\cdot}K$
k_B = biomass thermal conductivity, W/m·K
k_{0j} = pre-exponential factor of the j^{th} reaction, s^{-1}
k_j = Arrhenius-type kinetic rate constant of the j^{th} reaction, s^{-1}
K_{WGS} = equilibrium constant for water−gas shift reaction, -
L_{bed} = dense bubbling bed height, m
L_0 = bed height at minimum fluidization condition, m
$\dot{m}$ = mass flow rate, kg/s
M_{Char} = char hold-up inside reactor, kg
MW = molecular weight, g/mol
N_{or} = number of holes in the distributor plate, -
P = reactor pressure/total pressure inside particle, Pa
P_i = partial pressure of ith species, Pa or bar
R = reaction rate, s^{-1} or $mol/m^3{\cdot}s$
R = Universal ideal gas constant, 8.314 J/mol·K
R_p = spherical biomass particle radius, m
T = temperature, K
$_U$ = superficial gas velocity, m/s
U_0 = inlet gas velocity, m/s
w = mass fraction, -
$w_{j,i}$ = mass fraction of jth element in species i, -
W_{bed} = solids bed inventory, kg
y_i = mole fraction of ith species, -
$\overline{Y}$ = average yield, kg/kg dry biomass
$\overline{Y}_{H_2O,pyro}$ = pyrolytic water yield, kg/kg dry biomass
Z = axial coordinate along the reactor height, m

Greek

γ_i = stoichiometric coefficient of ith species in tar cracking reaction, -
ΔH^o_{rxn} = heat of reaction at standard condition, kJ/mol
$\Delta H_{rxn,j}$ = heat of jth reaction, kJ/kg
ε = bed voidage at height z, -
$\overline{\varepsilon}$ = average bubbling bed voidage, -
ε_{fb} = freeboard voidage, -
ρ = density, kg/m^3
τ_g = gas residence time, s
τ_P = mean solids residence, s

Subscripts

B = biomass
C = char, carbon
Fb = freeboard
G = noncondensable gas
H = hydrogen
I = species number
In = input to reactor
j = reaction number, element number
M = moisture
mf = minimum fluidization
O = oxygen

DOI: 10.1021/acs.energyfuels.6b03161
Energy Fuels 2017, 31, 1702−1711

P = particle
Pyro = pyrolysis
T = tar
V = water vapor

Abbreviations

BFB = bubbling fluidized bed
daf = dry-ash-free
WGS = water−gas shift
SMR = steam methane reforming

REFERENCES

(1) Edenhofer, O.; Pichs-Madruga, O.; Sokona, Y.; Seyboth, K.; Matschoss, P.; Kadner, S.; Zwickel, T.; Eickemeier, P.; Hansen, G.; Schlömer, S.; von Stechow, C. *IPCC Special Report on Renewable Energy Sources and Climate Change Mitigation*; Cambridge University Press: Cambridge, New York, 2011.

(2) Corella, J.; Toledo, J. M.; Molina, G. A review on dual fluidized-bed biomass gasifiers. *Ind. Eng. Chem. Res.* **2007**, *46*, 6831−6839.

(3) Ahmed, T. Y.; Ahmad, M. M.; Yusup, S.; Inayat, A.; Khan, Z. Mathematical and computational approaches for design of biomass gasification for hydrogen production: A review. *Renewable Sustainable Energy Rev.* **2012**, *16*, 2304−2315.

(4) Schuster, G.; Loffler, G.; Weigl, K.; Hofbauer, H. Biomass steam gasification − an extensive parametric modeling study. *Bioresour. Technol.* **2001**, *77*, 71−79.

(5) Gómez-Barea, A.; Leckner, B. Modeling of biomass gasification in fluidized bed. *Prog. Energy Combust. Sci.* **2010**, *36*, 444−509.

(6) LV, P. M.; Xiong, Z. H.; Chang, J.; Wu, C. Z.; Chen, Y.; Zhu, J. X. An experimental study on biomass air−steam gasification in a fluidized bed. *Bioresour. Technol.* **2004**, *95*, 95−101.

(7) Gil, J.; Aznar, P. M.; Caballero, A. M.; Frances, E.; Corella, J. Biomass gasification in fluidized bed at a pilot scale with steam-oxygen mixtures. Product distribution for very different operating conditions. *Energy Fuels* **1997**, *11*, 1109−1118.

(8) Ruoppolo, G.; Miccio, F.; Brachi, P.; Picarelli, A.; Chirone, R. Fluidized bed gasification of biomass and biomass/coal pellets in oxygen and steam atmosphere. *Chem. Eng. Trans.* **2013**, *32*, 595−600.

(9) Sikarwar, V. S.; Zhao, M.; Clough, P.; Yao, J.; Zhong, X.; Memon, M. Z.; Shah, N.; Anthony, E.; Fennell, P. An overview of advances in biomass gasification. *Energy Environ. Sci.* **2016**, *9*, 2939−2977.

(10) Gil, J.; Corella, J.; Aznar, M. P.; Caballero, M. A. Biomass gasification in atmospheric and bubbling fluidized bed: effect of the type of gasifying agent on the product distribution. *Biomass Bioenergy* **1999**, *17*, 389−403.

(11) Ammendola, P.; Chirone, R.; Miccio, F.; Ruoppolo, G.; Scala, F. Devolatilization and attrition behavior of fuel pellets during fluidized-bed gasification. *Energy Fuels* **2011**, *25*, 1260−1266.

(12) Li, X. T.; Grace, J. R.; Lim, C. J.; Watkinson, A. P.; Chen, H. P.; Kim, J. R. Biomass gasification in a circulating fluidized bed. *Biomass Bioenergy* **2004**, *26*, 171−193.

(13) Corella, J.; Sanz, A. Modeling circulating fluidized bed biomass gasifiers: A pseudo-rigorous model for stationary state. *Fuel Process. Technol.* **2005**, *86*, 1021−1053.

(14) Radmanesh, R.; Chaouki, J.; Guy, C. Biomass gasification in a bubbling fluidized bed reactor: experiments and modeling. *AIChE J.* **2006**, *52*, 4258−4272.

(15) Lü, P.; Kong, X.; Wu, C.; Yuan, Z.; Ma, L.; Chang, J. Modeling and simulation of biomass air-steam gasification in a fluidized bed. *Front. Chem. Eng. China* **2008**, *2*, 209−213.

(16) Kaushal, P.; Abedi, J.; Mahinpey, N. A comprehensive mathematical model for biomass gasification in a bubbling fluidized bed reactor. *Fuel* **2010**, *89*, 3650−3661.

(17) Li, X. Biomass gasification in a circulating fluidized bed. Ph.D. Thesis, University of British Columbia, 2002.

(18) Dupont, C.; Boissonnet, G.; Seiler, J. M.; Gauthier, P.; Schweich, D. Study about the kinetic processes of biomass steam gasification. *Fuel* **2007**, *86*, 32−40.

(19) Hamel, S.; Krumm, W. Mathematical modelling and simulation of bubbling fluidised bed gasifiers. *Powder Technol.* **2001**, *120*, 105−112.

(20) Fiaschi, D.; Michelini, M. A two-phase one-dimensional biomass gasification kinetics model. *Biomass Bioenergy* **2001**, *21*, 121−132.

(21) Thunman, H.; Niklasson, F.; Johnsson, F.; Leckner, B. Composition of volatile gases and thermo-chemical properties of wood for modeling of fixed or fluidized beds. *Energy Fuels* **2001**, *15*, 1488−1497.

(22) Pyle, D.; Zaror, C. Heat transfer and kinetics in the low temperature pyrolysis of solids. *Chem. Eng. Sci.* **1984**, *39*, 147−158.

(23) Murzin, D. Y. *Chemical Engineering for Renewables Conversion*; Academic Press, 2012.

(24) Ji, P.; Feng, W.; Chen, B. Comprehensive simulation of an intensified process for H_2 production from steam gasification of biomass. *Ind. Eng. Chem. Res.* **2009**, *48*, 3909−3920.

(25) Kunii, D.; Levenspiel, O. *Fluidization Engineering*, 2nd ed.; Butterworth, Boston, 1991.

(26) Yang, W. C. *Handbook of Fluidization and Fluid-Particle Systems*; Marcel-Dekker Inc. and Taylor & Francis Group LLC, 2003.

(27) Kaushal, P.; Abedi, J. A simplified model for biomass pyrolysis in a fluidized bed reactor. *J. Ind. Eng. Chem.* **2010**, *16*, 748−755.

(28) Liden, A. G.; Berruti, F.; Scott, D. S. A kinetic model for the production of liquids from the flash pyrolysis of biomass. *Chem. Eng. Commun.* **1988**, *65*, 207−221.

(29) Grønli, M. G.; Melaaen, M. C. Mathematical model for wood pyrolysis: comparison of experimental measurements with model predictions. *Energy Fuels* **2000**, *14*, 791−800.

(30) Shafizadeh, F.; Chin, P. P. S. Wood Technology: Chemical Aspects. In *American Chemical Society Symposium Series*; Goldstein, I. S., Ed.; American Chemical Society: Washington, DC, 1977; Vol. *43*, 57.

(31) Chan, W. C. R.; Kelbon, M.; Krieger, B. B. Modelling and experimental verification of physical and chemical processes during pyrolysis of a large biomass particle. *Fuel* **1985**, *64*, 1505−1513.

(32) Hejazi, B.; Grace, J. R.; Bi, X.; Mahecha-Botero, A. Coupled reactor and particle model of biomass drying and pyrolysis in a bubbling fluidized bed reactor. *J. Anal. Appl. Pyrolysis* **2016**, *121*, 213−229.

(33) Di Blasi, C.; Branca, C. Kinetics of primary product formation from wood pyrolysis. *Ind. Eng. Chem. Res.* **2001**, *40*, 5547−5556.

(34) Sutton, D.; Kelleher, B.; Ross, J. R. H. Review of literature on catalysts for biomass gasification. *Fuel Process. Technol.* **2001**, *73*, 155−73.

(35) Boroson, M. L.; Howard, J. B.; Longwell, J. P.; Peters, W. A. Product yields and kinetics from the vapor phase cracking of wood pyrolysis tars. *AIChE J.* **1989**, *35*, 120−128.

(36) Rapagnà, S.; Jand, N.; Kiennemann, A.; Foscolo, P. U. Steam-gasification of biomass in a fluidized-bed of olivine particles. *Biomass Bioenergy* **2000**, *19*, 187−197.

(37) Barrio, M.; Hustad, J. E. CO_2 gasification of birch and the effect of CO inhibition on the calculation of chemical kinetics. In *Progress in Thermochemical Biomass Conversion*; Bridgwater, A. V., Ed.; Blackwell Science Ltd.: Oxford, U.K., 2001.

(38) Barrio, M.; Gobel, B.; Risnes, H.; Henriksen, U.; Hustad, J.; Sorensen, L. Steam gasification of wood char and the effect of hydrogen inhibition on the chemical kinetics. In *Progress in Thermochemical Biomass Conversion*; Bridgwater, A. V., Ed.; Blackwell Science Ltd.: Oxford, U.K., 2001.

(39) Babu, B.; Sheth, P. Modeling and simulation of reduction zone of downdraft biomass gasifier: effect of char reactivity factor. *Energy Convers. Manage.* **2006**, *47*, 2602−2611.

(40) Gómez-Barea, A.; Leckner, B. Estimation of gas composition and char conversion in a fluidized bed biomass gasifier. *Fuel* **2013**, *107*, 419−443.

(41) Biba, V.; Macak, J.; Klose, E.; Malecha, J. Mathematical modeling for the gasification of coal under pressure. *Ind. Eng. Chem. Process Des. Dev.* **1978**, *17*, 92−98.

DOI: 10.1021/acs.energyfuels.6b03161
Energy Fuels 2017, 31, 1702−1711

(42) Parent, J. D.; Katz, S. Equilibrium compositions and enthalpy changes for the reaction of carbon, oxygen, and steam. *Research Bulletin 2*; IGT-Inst. Gas Tech., 1948.
(43) Oasmaa, A.; Meier, D. In *Fast Pyrolysis of Biomass: A Handbook*; Bridgwater, A.V., Ed.; CPL Press, 2002; p 23.
(44) Neves, D.; Thunman, H.; Matos, A.; Tarelho, L.; Gómez-Barea, A. Characterization and prediction of biomass pyrolysis products. *Prog. Energy Combust. Sci.* **2011**, *37*, 611−630.
(45) Clift, R.; Grace, J. R. *Continuous bubbling and slugging, Fluidization*; Academic Press: London, 1985; pp 73−132.
(46) Darton, R. C.; Lanauze, R. D.; Davidson, J. F.; Harrison, D. Bubble growth due to coalescence in fluidized-beds. *Trans. Inst. Chem. Eng.* **1977**, *55*, 274−280.
(47) Herguido, J.; Corella, J.; González-Saiz, J. Steam gasification of lignocellulosic residues in a fluidized bed at a small pilot scale. Effect of the type of feedstock. *Ind. Eng. Chem. Res.* **1992**, *31*, 1274−1282.
(48) Asadi-Saghandi, H.; Sheikhi, A.; Sotudeh-Gharebagh, R. Sequence-based process modeling of fluidized bed biomass gasification. *ACS Sustainable Chem. Eng.* **2015**, *3*, 2640−2651.

DOI: 10.1021/acs.energyfuels.6b03161
Energy Fuels 2017, 31, 1702−1711